Materials Science in Semiconductor Processing 24 (2014) 50–56

Contents lists available at ScienceDirect

Materials Science in Semiconductor Processing

journal homepage: www.elsevier.com/locate/mssp

Development of oxide based window and buffer layer for single junction amorphous solar cell: Reduction of light induced degradation

Gourab Das [b], Sourav Mandal [b], M. Rajive Tomy [a,*], Chandan Banerjee [a], Sumita Mukhopadhyay [b], A.K. Barua [b]

[a] HHV Center for Advanced Photovoltaic Technologies Pvt. Ltd., Peenya Industrial Area, Bangalore 560058, India
[b] Centre of Excellence for Green Energy and Sensor Systems, Bengal Engineering and Science University, Shibpur, Howrah 711103, India

ARTICLE INFO

Keywords:
Amorphous material
Semiconductor
Thin film
Plasma deposition

ABSTRACT

Single junction a-Si:H solar cell using oxide based window and buffer layer was fabricated by using a conventional plasma enhanced chemical vapor deposition (PECVD) technique. The impact of oxide based window layers and the effect of oxide buffer layer thickness on light induced degradation are investigated. Solar cells with optimized oxide based window and buffer layers have been fabricated with an optical gap of 1.97 eV and 1.86 eV. On comparing these solar cells with carbide based window and buffer layers, it is found that light induced degradation (LID) of oxide based cells is almost 4% less than the carbide based ones. Oxide based cells show significant improvement in quantum efficiency for lower wavelength region, compared to carbide based cells. Stabilized efficiency after 1000 h light soaking for the oxide and carbide based solar cells is found to be 7.55% and 6.50%, respectively.

© 2014 Elsevier Ltd. All rights reserved.

1. Introduction

Amorphous silicon (a-Si:H) as an absorber for thin film solar cells has fascinated the scientific community for last several decades. It remains as the material of choice for the advanced solar cell technology due to its flexibility in engineering the optical gap, inexpensive raw materials with low processing temperature and the scope for manufacture in large scale of large area substrates. On the downside this technology faces two major issues, one is the low conversion efficiency and the other is the light induced degradation. In order to increase the stabilized efficiency of a single junction amorphous silicon solar cell, researchers have devised different approaches, such as incorporation of nano-crystallites in intrinsic a-Si:H films [1], improvement of window and buffer layer qualities, etc. [2–7]. The quality of window layer material and the layer thickness play a significant role in enhancing the shorter wavelength quantum efficiency [8]. In order to improve the overall conversion efficiency of solar cells, the individual layers, i.e. window and intrinsic layers, with superior quality are an essential prerequisite. Moreover, from device point of view, the *p*/*i* interface also plays a vital role in reducing bandgap mismatch and thus reduces the recombination of charge carriers. The recombination centers or trap centers at the interface arise from internal electric field distribution due to localized states. In the conventional hydrogenated amorphous silicon carbide (a-SiC:H) window layer material [9], it is generally observed that with increase in carbon incorporation, the bandgap increases at the cost of dark conductivity, photoconductivity and mobility lifetime product ($\mu\tau$) [10,11]. This results in increased dangling bond density and bonded hydrogen content in the film [11,12].

* Corresponding author. Tel.: +91 80 41931115; fax: +91 80 28394874.
E-mail address: rajivetomy@hhv.in (M.R. Tomy).

http://dx.doi.org/10.1016/j.mssp.2014.03.009
1369-8001/© 2014 Elsevier Ltd. All rights reserved.

Recent studies on hydrogenated amorphous silicon oxide (a-SiO:H) revealed it as a superior photovoltaic material compared to the conventional a-SiC:H [13–15]. The fundamental advantage of using a-SiO:H films is that they provide higher optical gap retaining more or less the same photoconductivity of a-SiC:H. This is due to the two phase structure of a-SiO:H where islands of SiO are embedded within the matrix of a-Si:H [16]. The Si:H part contributes to the conductivity whereas the SiO part provides the optical gap. Since the matrix is a-Si:H, the dopability of a-SiO:H film is expected to be high. However, obtaining better quality oxide material is always challenging as the electronic and optical properties depend considerably on process parameters and the overall oxygen incorporation into the a-Si:H network [13]. Fujiwara et al. [17] have shown the successful application of a-SiO:H material in their heterojunction solar cells for efficiency improvement.

In our present work we fabricated superior quality a-SiO:H film for p and buffer layers for a single junction a-Si:H solar cell using the conventional plasma enhanced chemical vapor deposition (PECVD) process. The buffer layers used in the study were advantageous, as they passivate or improve the quality of the junction and control the recombination of minority carriers in doped a-Si:H, which in turn improves the open circuit voltage. Moreover, the influence of oxide based window and buffer layers on the initial efficiency and light induced degradation (LID) of single junction a-Si cell was studied in comparison with carbide based cell.

2. Experimental

Silicon oxide based material (a-SiO:H) and single junction a-Si solar cells were developed using seven chambers inline Radio Frequency Plasma Enhanced Chemical Vapor Deposition (RF-PECVD, 13.56 MHz) systems. Different layers like p, buffer, i and n were deposited in different chambers. Isolation chambers were used in between the doped and undoped process chambers, to avoid cross contamination. The gap between the RF electrode and substrate was 15 mm. Semiconductor grade purity gases such as silane (SiH_4), hydrogen (H_2), carbon-dioxide (CO_2) and methane (CH_4) were used for the development of oxide and carbide based hydrogenated amorphous silicon films (a-SiO:H, a-SiC:H). To make p-type films diborane (B_2H_6) was used (diborane 1% in He). Flow ratio of CO_2 to SiH_4, (CO_2/SiH_4) was varied from 0.75 to 1.25, hydrogen dilution (H_2/SiH_4) varied from 15 to 30, power density was varied from 40 mW/cm^2 to 50 mW/cm^2, chamber pressure varied from 1 to 1.5 Torr and substrate temperature was kept constant at 200 °C. Sodium potassium free glasses were used as substrates in order to develop the silicon oxide/carbide materials. The optoelectronic and structural characteristics of both oxide and carbide based buffer layers were studied by varying the process parameters as well as layer thickness. Thicknesses of the films were measured using a stylus profiler (Dektak 6M). Absorbance spectra of the films were measured by an UV–vis–NIR spectrophotometer (Shimadzu-UV 1700) and the optical band gaps were calculated from absorbance spectra using Tauc plot and the equation given below

$$(\alpha h\nu)^{1/2} = B^{1/2}(h\nu - E_g), \tag{1}$$

where $h\nu$ is the energy, α is the optical absorption coefficient, E_g is the optical gap and B is a constant ($\sim 10^5$ cm^{-1} eV^{-1}) [18].

Steady state photoconductivity was measured under 100 mW/cm^2 white light from a tungsten lamp. The activation energy of films has been measured by studying the dark conductivity as a function of temperature. The temperature dependent dark conductivity (σ_D) of a given sample is given by the well established Arrhenius relation, which is expressed as

$$\sigma_D = \sigma_0 \exp[-E_a/kT] \quad (S\,\mathrm{cm}^{-1}), \tag{2}$$

where σ_0 is the conductivity pre-factor, E_a is the thermal activation energy, k is the Boltzmann constant and T is the temperature in Kelvin. This relation is also used to determine the activation energy from the slope of ln σ_D vs. $10^3/T$ plot.

Conductivity measurements were carried out in a cryostat, consisting of a chamber with evacuation arrangement and a heating system. The chamber vacuum of $\sim 10^{-5}$ Torr was attained with the help of a turbo pump. A copper block holder was used to mount the samples using silver paint, enabling good thermal contact and a heating coil was attached to attain the desired temperature for the sample. Ohmic contacts were made to the co-planar aluminum electrodes of the sample under test and the terminals of an electrometer (Keithley, 6487) that applies the voltage as well as measures the current flowing through the sample were connected. The magnitude of the applied voltage depends upon the nature of the sample. All the samples were annealed in vacuum at 150 °C for 1 h prior to the measurement in order to avoid any effect of absorbed gases. The sample was then cooled down slowly in a stepwise manner and the conductivity was measured at each step.

Bonded hydrogen and oxygen contents were studied using Fourier transform infrared spectroscopy (Shimadzu IRAffinity-1). Atomic percent of oxygen C(O) incorporated in the film is obtained from the integrated absorption strength of IR absorption in the range of 900–1200 cm^{-1}, and it is found to be 34%. The total bonded oxygen, (N_O) can be calculated from the area under the absorption peak centered between 960 and 1080 cm^{-1}.

$$N_O = A(O)\int(\alpha/\omega)d\omega, \tag{3}$$

where α is the absorption coefficient, ω is the frequency in cm^{-1}. A(O) is the calibration factor [19].

Light induced degradation of the films was measured under AM 1.5 light isolation at a room temperature (50 °C) for 1000 h under 1 sun condition.

Solar cells were fabricated on TCO (SnO_2:F, AFG C type) coated glass substrate with two structures: glass/TCO/p-a-SiC:H/i-a-SiC:H/i-a-Si:H/n-a-SiH/ZnO/Al for carbide based cell and glass/TCO/p-a-SiO:H/i-a-SiO:H/i-a-Si:H/n-a-Si:H/ZnO/Al for oxide based cell. In order to optimize the efficiency of the solar cell i-layers of different thicknesses (2000 Å, 2500 Å and 3000 Å) buffer layers of different

thickness (50 Å, 70 Å, 90 Å and 100 Å) were used. Back contacts of solar cells were made with ZnO/Al with electrode area of 1 cm^2. ZnO back reflector layer and Al back contact were deposited by DC magnetron sputtering. $I-V$ characteristics of the solar cells produced were measured by a solar simulator under AM 1.5, i.e. 100 mW/cm^2 light intensity. The spectral response was measured by using Spectronova SNSR-XS 130BC.

3. Results and discussions

Investigations on the influence of CO_2/SiH_4 and H_2/SiH_4 ratios on p-type and intrinsic buffer layers were carried out by varying the process parameters. Optimized process parameters used for the deposition of intrinsic and boron doped a-SiO:H films are shown in Table 1. Optoelectronic and structural properties with the optimized process parameter for oxide based buffer layer are depicted in Table 2. In order to make a comparative study, the optoelectronic and structural properties of carbide based buffer layer are also included in Table 2. It is clear from data shown in Table 2 that, for given bandgap value, oxide based buffer layer has one order gain more than that of carbide buffer. Oxide film has initial dark conductivity of $\sim 10^{-11}$ S cm^{-1}, and therefore it is less defective. In the case of oxide material, the bandgap obtained is ~1.86 eV and for these materials the locations of the Fermi level will be near the midgap position, i.e. 0.9 eV. The activation energy data of oxide films shown in Table 2 (0.86 eV) is much closer to the Fermi level position than that of carbide buffer (0.78 eV). The difference in activation energy of carbide layer and oxide is found to be only 0.08 eV even though there is a one order difference between their dark conductivity values. The reason for low dark conductivity values for oxide layers compared to carbide ones may be due to fewer defects or due to high activation energies in a-SiO:H [17]. In the case of oxide films, oxygen is not uniformly distributed in the film due to the two phase structure but in the case of carbide layer, carbon is uniformly distributed over the film resulting in a higher defect compared to the oxide [16].

These facts altogether show that use of oxide buffer in the single junction a-Si:H solar cell is more advantageous than that of carbide buffer. The band diagram and structure of the oxide cells are shown in Fig. 1(a) and (b), respectively.

Studies on light induced degradation of individual oxide and carbide based buffer layers have been carried out for 1000 h and results are shown in Fig. 2. It has been observed that in the initial condition both dark- and photo-conductivities are less for oxide based material than for carbide based material. The initial σ_d is $\sim 10^{-11}$ S cm^{-1} for intrinsic oxide materials. It is clear from Fig. 2 that the degradation of the oxide based material is less compared to that of the carbide based material. A reason for this could be the fewer defects within the oxide film. As a-SiO:H is a two phase material, where SiO is embedded within the a-Si:H matrix, the defects created within the film for alloying with oxygen are less compared to alloying with carbide. This two phase nature of oxide based material gives better optoelectronic properties. All these facts establish that oxide is a better material for use as a buffer layer in p/i interface.

Solar cells fabricated with the optimized oxide based p and buffer layers are mentioned in Table 2, by keeping the absorber layer thickness 2500 Å (optimized absorber layer thickness for carbide based solar cell). Initially the thickness dependence of buffer layer on solar cell output has been studied. Buffer layer thickness is varied from 50 to 100Å . Table 3 shows the results of the dependence of buffer layer thickness on different PV parameters. It is clear from the Table 3 that 70 Å is the optimum buffer layer thickness to attain highest stabilized efficiency. Both open circuit voltage and fill factor have been maximized to 0.87 V and 0.7, respectively on applying buffer layer thickness of 70 Å. At this thickness of buffer layer recombination defects and trap centers reduce at the p/i interface. So a better carrier collection and electrical field distribution are possible [6]. As the thickness of buffer layer increases further, the efficiency decreases as the tunneling of carriers gets hindered after buffer layer thickness of 70 Å.

It is known that performance of the solar cell is highly dependent on the thickness of absorber or active layer. In order to study the influence of thickness of active layer on cell performance, we have deposited cells having i-layer thickness of 2000 Å, 2500 Å and 3000 Å. Different photovoltaic (PV) parameters and their light induced degradation with i-layer thickness are shown in Table 4. As i-layer thickness of a-Si:H cell is increased from 2000 Å to 2500 Å overall cell efficiency improves from 8.8% to 9.18% due to the increase in current density from 14.1 mA/cm^2 to

Table 1
Optimized process parameters for the deposition of intrinsic and boron doped a-SiO:H films.

Sample no.	Material	H_2/SiH_4	B_2H_6 (1% in He)	CO_2/SiH_4	Power density (mW/cm^2)	Operating pressure (Torr)	Deposition rate (°/min)
546-P	p- a-SiO:H	30	9	0.916	30	1.5	45
548-I	i-a-SiO:H	20	NA	0.2	25	1.0	56

Table 2
Comparison of optoelectronic properties for the optimized process parameter for different buffer layers.

Sample Id	Material type	Dark conductivity, σ_d (S cm^{-1})	Photoconductivity, σ_{ph} (S cm^{-1})	Oxygen content C (O) (at%)	Hydrogen content C (H) (at%)	Bandgap (E_g) (eV)	Activation energy (E_{act})
345-I	a-SiC:H	4.2×10^{-10}	1.8×10^{-5}	NA	10.8	1.84	0.78
548-I	a-SiO:H	4.0×10^{-11}	8.2×10^{-6}	5.3	11.0	1.86	0.86

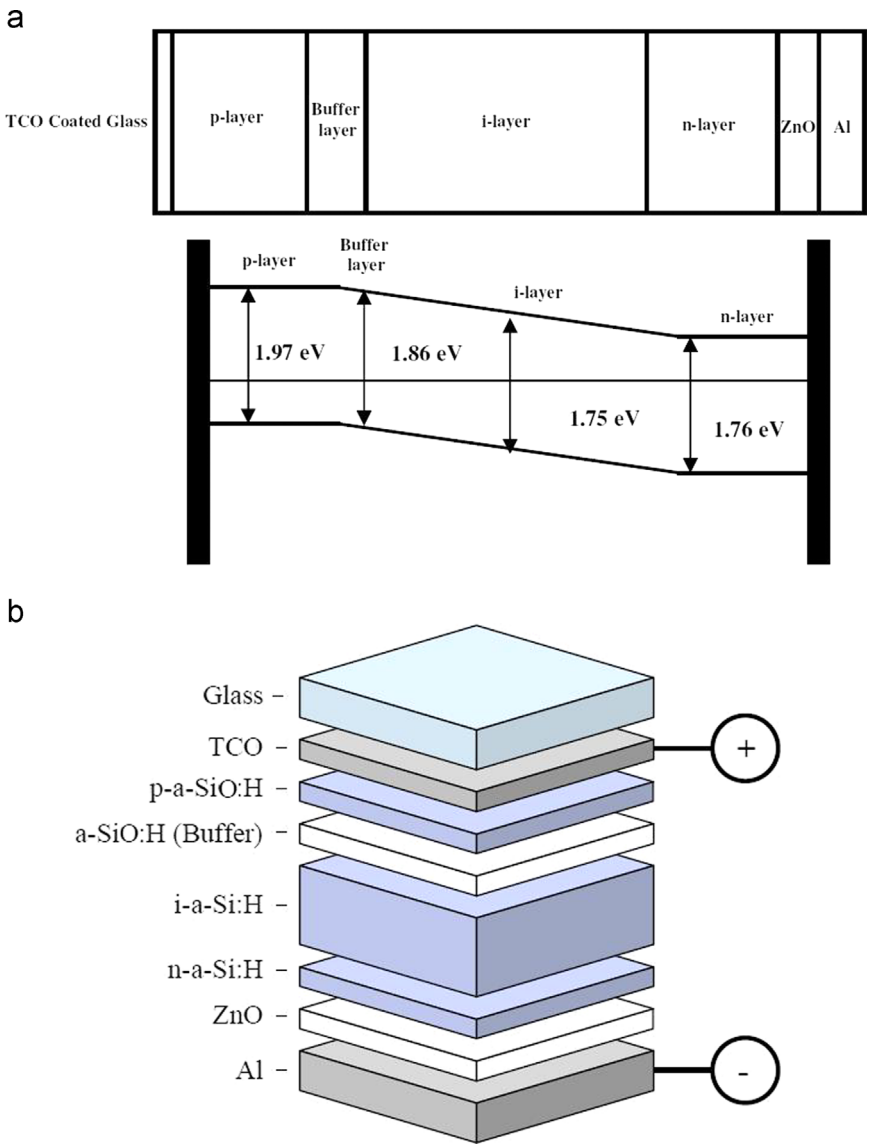

Fig. 1. (a) Band diagram and (b) structure of the thin film amorphous silicon solar cell.

15.0 mA/cm^2. The light induced degradation also increases from 14.5% to 17% and as a result stabilized efficiency remains more or less the same. In the case of oxide based window layer one can go to higher optical gap ($\sim$1.98 eV) retaining the higher conductivity compared to other alloys like carbide ($\sim$1.90 eV) counterpart. This allows more light into the cell and gives higher conversion efficiency. When absorber layer thickness was reduced from 2500 Å to 2000 Å, the stabilized conversion efficiency did not change much, because current density change was less compared to that of carbide based cell. This may be due to better blue response of the cell which gives better current in spite of less absorber layer thickness. This is one of the advantages of using oxide based window and buffer layer where it is possible to keep the absorber layer thickness less without compromising much with stabilized conversion efficiency. As the absorber layer thickness increased further to 3000 Å, the initial efficiency increases but the stabilized efficiency reduces. As the absorber layer thickness increases, the efficiency increases because more light will be absorbed as well as light induced degradation also increases. So in this work the optimized absorber layer thickness is 2500 Å where more stabilized efficiency has been used.

To show the superiority of oxide based solar cell over the conventional carbide based solar cell, we have fabricated the carbide based solar cell and optimized data along with its degraded values are shown in Fig. 3. It is found that the same 70 Å is the optimum thickness required for the buffer layer like oxide based cell. The optimum thickness of the intrinsic layer for this solar cell was 2500 Å to achieve the highest stabilized efficiency. The solar cells fabricated under optimized window and buffer condition showed initial conversion efficiency, η of 8.3%; V_{oc}=0.83 V, J_{sc}=13.75 mA/cm^2 and FF=0.72 have been achieved from

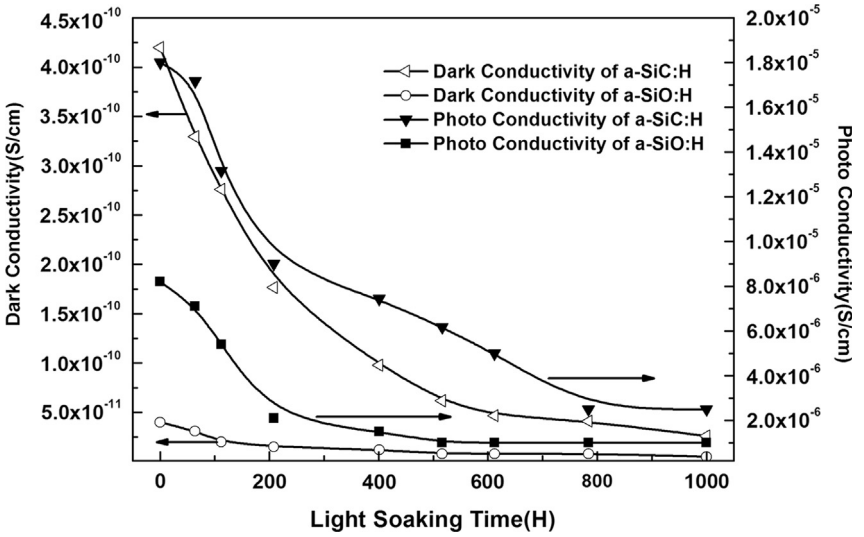

Fig. 2. Light induced degradation of dark- and photo-conductivities for the carbide and oxide films.

Table 3
PV parameters with different buffer layer thicknesses (absorber layer thickness 2500Å).

Cell ID	Buffer layer thickness (Å)	J_{sc} (mA/cm^2)	V_{oc} (V)	FF	Initial η	LID (%)	Stable η
486	0	14.95	0.80	0.7	8.37	16.5	6.99
521	50	15.12	0.82	0.70	8.68	17.2	7.18
544	**70**	**15.01**	**0.87**	**0.70**	**9.18**	**17.7**	**7.55**
549	90	14.96	0.85	0.69	8.77	18.0	7.19
561	100	14.89	0.85	0.68	8.60	18.4	7.02

Table 4
PV parameters with degradation for different absorber layer thicknesses.

Cell ID	Absorber layer thickness (Å)	J_{sc} (mA/cm^2)	V_{oc} (V)	FF	Initial η	LID (%)	Stable η
556	2000	14.41	0.86	0.71	8.80	14.5	7.52
544	2500	15.01	0.87	0.7	9.18	17.7	7.55
561	3000	15.57	0.86	0.7	9.37	22.5	7.26

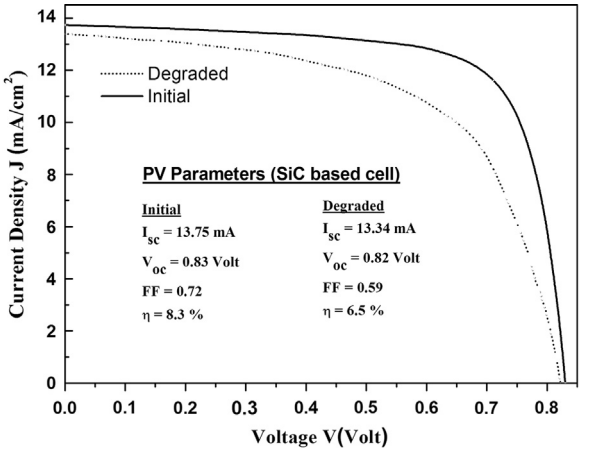

Fig. 3. *J–V* characteristics of a carbide based p–i–n single junction solar cell at initial and light soaked conditions.

the cell using buffer layer optical gap (E_{opt})=1.84 eV. Other properties of the above mentioned buffer layer are shown in Table 2. Fig. 4 shows the normalized degradation of PV parameters for carbide based cells. It is found that the typical degradation for carbide based cells is V_{oc}=1.2%, J_{sc}=2.98%, FF=18.05% and η=21.6%. The reduction of efficiency is mainly influenced by the drop in fill factor.

Single junction solar cells have been fabricated using oxide based window and buffer layer instead of using conventional carbide based window and buffer layers. Fig. 5 shows the *J–V* characteristics of the oxide based solar cell at initial and light soaked conditions. It is observed that at initial condition the highest efficiency obtained by this cell is 9.18%, J_{sc}=15.01 mA/cm^2, V_{oc}=0.87 V, FF=0.70. After 1000 h of light soaking efficiency decreased to 7.55%, J_{sc}=14.51 mA/cm^2, V_{oc}=0.86 V, FF=0.61. Fig. 6 shows the normalized degradation of PV parameters for the oxide based cells. It is also observed that like carbide based cell, fill factor of oxide based cell degrades maximum. If we compare the light induced degradation of oxide based cells with that of carbide based cells, it is found that the light induced degradation of these cells is almost 4.0% (LID: 21.6 and 17.7%) less than that of the carbide based cells.

Fig. 7 shows the comparison of absorption coefficient (α) with different energies ($h\nu$) for the carbide and oxide based window layer. It is clear from Fig. 7 that the oxide based window layer has higher absorption compared to the carbide one. Fig. 8 shows the comparison of quantum efficiencies of carbide and oxide based solar cells after light soaking for ~1000 h. It is very clear from the graph that oxide based cells show superior blue response compared to carbide based solar cells. The difference in short circuit current of the oxide and carbide based cells for the same absorber layer thickness can be explained from Fig. 8. Oxide based cells show 9% more current density compared to carbide based cells for 2500 ° absorber layer.

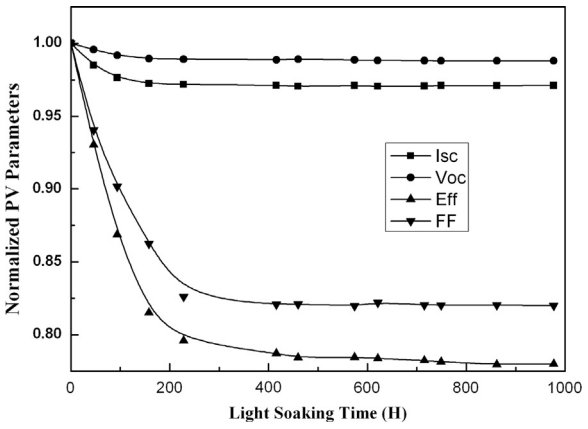

Fig. 4. Normalized PV parameters of carbide based p–i–n single junction solar cell after 1000 h of light soaking.

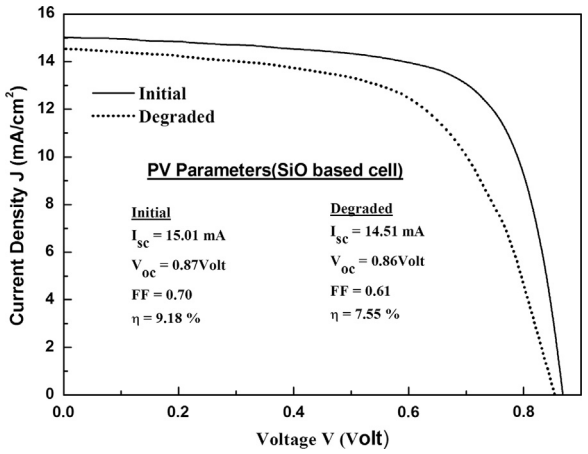

Fig. 5. *J–V* characteristics of an oxide based p–i–n single junction solar cell at initial and light soaked conditions.

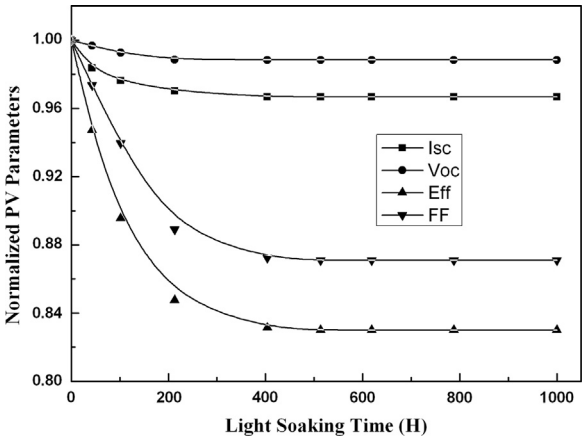

Fig. 6. Normalized PV parameters of the oxide based p–i–n single junction solar cell after 1000 h of light soaking.

Fig. 8 shows that by using oxide based buffer layer, i.e. by improving the p/i interface the quantum efficiency between 300 and 550 nm wavelength regions of the solar

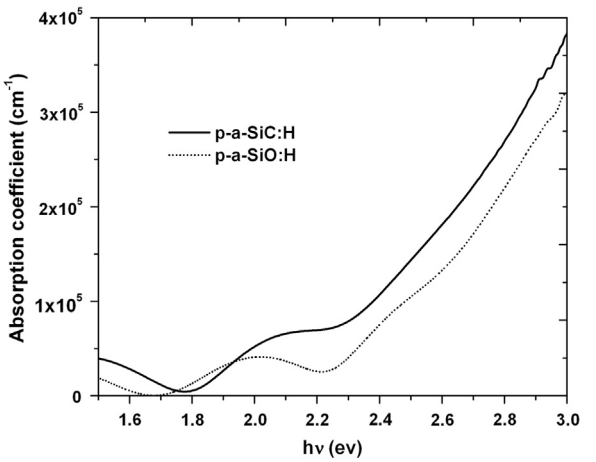

Fig. 7. Variation of absorption coefficient (α) with different energies ($h\nu$) for different window layers.

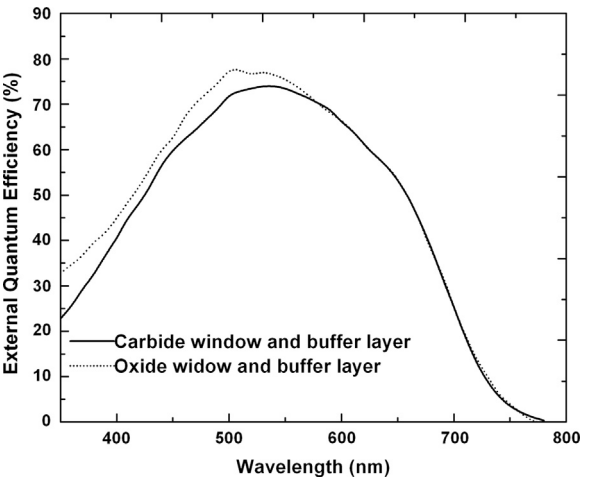

Fig. 8. Comparison of the external QE for the oxide and carbide based solar cells.

spectrum is improved. It may be due to the fact that oxide based window and buffer layers allow more blue part of the spectrum within the cell resulting in enhancement in blue response. It is also observed from the graph that the solar cell response in the lower wavelength region mainly depends on the window and buffer layer properties.

This study shows the superiority of oxide based window and buffer layers in single junction amorphous silicon based solar cells compared to the conventional carbide based solar cells. The superior results obtained with the oxide based small area cells motivated us to fabricate monolithic minimodule and result of this experiment will be communicated in the next paper.

4. Conclusions

Device quality oxide based window and buffer layers have been developed by the RF-PECVD method for the fabrication of single junction amorphous silicon based thin film solar cells. The superiority of oxide based solar cells

compared to the conventional carbide based solar cell has been demonstrated. By using a-SiO:H based window and buffer layers, solar cell efficiency improved by 16.5% compared to conventional carbide based solar cell. The thickness dependence of buffer and absorber layers has also been studied to get the optimum output. Intrinsic and buffer layer thicknesses have been optimized to be 2500 Å and 70 Å, respectively. Highest stabilized solar cell conversion efficiency of 7.55% has been obtained with light induced degradation limited to 17.7%. Reduction in absorber layer thickness to 2000 Å for oxide based solar cells shows a marginal decrease in stabilized conversion efficiency, which in turn can reduce the deposition time and material usage without compromising much in solar cell output.

Acknowledgment

Gourab Das gratefully acknowledge DST-INSPIRE Programme Division, India for the financial support.

References

[1] L. Raniero, L. Pereira, S. Zhang, I Ferreira, H. Aguas, E. Fortunable, R. Martins, J. Non-Cryst. Solids 338 (2004) 206.
[2] Y. Tawada, K. Tsuge, M. Kondo, H. Okamoto, Y. Hamakawa, Appl. Phys. Lett. 39 (1981) 237.
[3] Y. Tawada, K. Tsuge, M. Kondo, H. Okamoto, Y. Hamakawa, J. Appl. Phys. 53 (1982) 5273.
[4] K.S. Lim, M. Konagai, K. Takahashi, J. Appl. Phys. 56 (1984) 538.
[5] H. Sakai, T. Yoshida, S. Fujikake, T. Hama, Y. Ichikawa, J. Appl. Phys. 67 (1990) 3494.
[6] F.H. Karg: , in: Proceedings of the 20th IEEE Photovoltaic Solar Energy Conference, 1998, p. 149.
[7] H. Zhu S.J. and Fonash: , in: Proceedings of the 25th IEEE Photovoltaic Specialists Conference (PVSC), 1996, p. 1097.
[8] K. Ding, U. Aeberhard, F. Finger, U. Rau, Phys. Status Solidi – Rapid Res. Lett. 6 (2012) 193.
[9] Y. Tawada, M. Kondo, H. Okamoto and Y. Hamakawa: , in: Proceedings of the 15th IEEE Photovoltaic Specialists Conference, 1981, p. 245.
[10] Y. Tawada, M. Kondo, H. Okamoto, Y. Hamakawa, Sol. Energy Mater. 6 (1982) 299.
[11] A. Morimoto, T. Mitmura, M. Kumeda, T. Shimizu, J. Appl. Phys. 53 (1982) 7299.
[12] K. Nakagawa, S. Ueda, M. Kumeda, A. Moromoto, T. Shimizu, Jpn. J. Appl. Phys. 21 (1982) L176.
[13] S. Fujikake, H. Ohta, A. Sano, Y. Ichikawa, H. Sakai, Mater. Res. Soc. Symp. Proc. 258 (1992) 875.
[14] P. Sichanugrist, T. Sasaki, A. Asano, Y. Ichikawa, H. Sakai, Sol. Energy Mater. Sol. Cell 34 (1994) 415.
[15] A. Sarker, A.K. Barua, Jpn. J. Appl. Phys. 41 (2002) 765.
[16] H. Watanabe, K. Haga, T. Lohner, J. Non-Cryst. Solids 164–166 (1993) 1085.
[17] H. Fujiwara, T. Kaneko, M. Kondo, Appl. Phys. Lett. 91 (13) (2007).
[18] J. Tauc, Amorphous and Liquid Semiconductors, Plenum Press London, New York, 1974, 159.
[19] M. Zacharias, T. Drusedau, A. Panckow, H. Freistedt, B. Garke, J. Non-Cryst. Solids 169 (1994) 29.